

Evaluation of Light Distribution and the Penetration Depth under Isometric Studies using fNIRS

A.A.A. Halim^{1,3}, M.H. Laili², M. Rusop³

¹Faculty of Applied Sciences, Universiti Teknologi MARA (UiTM), 40450 Shah Alam, Selangor, Malaysia

²Photonics R&D, MIMOS Semiconductor Sdn Bhd, Technology Park Malaysia, 43300 Kuala Lumpur, Malaysia

³NANO-SciTech Centre, Institute of Science, Universiti Teknologi MARA (UiTM), 40450 Shah Alam, Selangor, Malaysia
amal.asyikin@gmail.com

Abstract— Functional near-infrared spectroscopy (fNIRS) has been widely used to solve the propagation of light inside the tissues and to quantify the oxygenation level of hemoglobin and myoglobin in human muscle. Penetration depth is one of the highlighted optical properties in this instrument in order to make sure light can be penetrated into deep human tissue layers. In this paper, our ultimate aim is to measure the penetration depth of muscle under different oxygenation states of isometric assessment in human using fNIRS. 27 sedentary healthy volunteers participated in this study. The result showed that, after all assessments, the mean signal of 3.0 and 4.0 cm distance of penetration depth showed more significant value detection ($p \leq 0.05$) measured by fNIRS. In addition, deoxygenated ($p = 0.031$) show more significant in gender analysis compare to the oxygenated and total of hemoglobin and myoglobin. Thus, this result may help us to prove that our human muscle is transparent to this near infrared region and might be a useful tool for detecting oxygen status in muscle from living people either athletes or working people.

Index Terms—fNIRS; Haemoglobin; Myoglobin; Penetration Depth.

I. INTRODUCTION

Penetration depth of human tissue is laterally related to a term called as 'optode'. Optode is actually the separation between source and detector located on devices called as near-infrared spectroscopy NIRS or functional near-infrared spectroscopy fNIRS [1]. Optode separation is important to estimate penetration depth over tissue layer [2]. Most studies tend to use optode separation with (2-4) cm [2-6]. But for muscle studies, the deepest penetration depth is 5 cm and this separation usually was specified for the upper arm and leg studies [3]. Multichannel is important to obtain signals from skeletal muscle independent of superficial tissue [4]. In addition, fat thickness information is important for wellbeing and future application in which it can confound readings of tissues that lie beneath [5]. To date, the source-detector distance has obtained in the range of optode 2.6-29 cm for fat measurement [5]. Optical lipid signal is a good predictor of adipose tissue thickness (ATT) less than 16 mm. The possibility of measuring ATT directly might be an efficient alternative to the measurement of ATT by ultrasound. The NIR signal intensity also can be influenced by optode separation [6]. It is said that, the overlying fat thickness of 5mm reduces the signal intensity by approximately 20 percent, with a light source-detector separation of 30-40mm. The use of shorter separation distances, 15-20mm, attenuates the signal by 30-60 per cent. Some studies reported that, the reduction signal is caused by the difference of absorption and scattering from each layer [7]. The higher the absorption, the

lower the penetration depth into deep layer [8]. More preliminary research study used four pulsed laser diodes at four wavelengths: 775, 810, 850, and 905 nm, whereas scattered light is detected by three photodiodes placed 5 cm away from the emitter [9]. Thus, optode positioning is important to assure appropriate penetration of photons to deep muscle, avoid stray, short path light and prevent recording primarily from more superficial structures.

This contribution of fat layer will affect the penetration depth of light into a deep layer of the muscle tissue [10]. The distance between source-detector and choice of source is the main factor which affects the light scattering and light propagation which only allows only a few cubic centimeters into the layer of superficial muscle. In addition, the problem still arises from a signal NIRS whether it was affected from the desaturation of myoglobin and the light scattering during exercises. This will increase the signal to noise ratio due to the vibration of the system upon the motion of human subjects while recording the signal.

In this study, we proposed a method to evaluate penetration depth of human muscle at different oxygenation states assessment in human flexor digitorum superficialis (FDS) muscle using fNIRS. Modified beer lambert's law will be used in order to build a better understanding of light absorption potential (LAP) between chromophores under tissue multilayers in human muscle [2]. Thus, by evaluating this optimum penetration depth, it could be useful tools for monitoring oxygenation state under human tissue during daily human activity.

II. METHODOLOGY

A. Subject Preparation

Fifty healthy volunteers from the sedentary group (age: 30 ± 10 years) were participated in this study and successfully completed the given questionnaire. Twenty-seven out of fifty healthy volunteers which having training 150 minutes per week were selected and agreed to continue with a non-invasive test using wireless Portalite fNIRS. All written informed consent from all 27 volunteers (16 males and 11 females) was obtained from Faculty of Health Science UiTM Puncak Alam and all protocols study was already approved by Research Management Institute (RMI). All volunteers are fully informed about the procedures and risks of the study.

B. Functional Near Infrared Spectroscopy

Portalite probe fNIRS devices with optode separation at 3.0 cm, 3.5 cm and 4.0 cm were positioned on the right human forearm at flexor digitorum superficialis (FDS) muscle regions [8-10]. This device was placed with a velcro

strap to avoid the noise of probe movement during all exercise activities [11].

Portalite is one of portable and wireless functional near-infrared spectroscopy manufactured from Artinis, Netherland [12][13]. This device is connected via Bluetooth to PC for collecting data and storage using Artinis’s dedicated software called as Oxysoft[14]. As illustrated in Figure 1, this device consists of 3 pairs of 760 nm and 830 nm sources (transmitters) with one detector (receiver) [15].

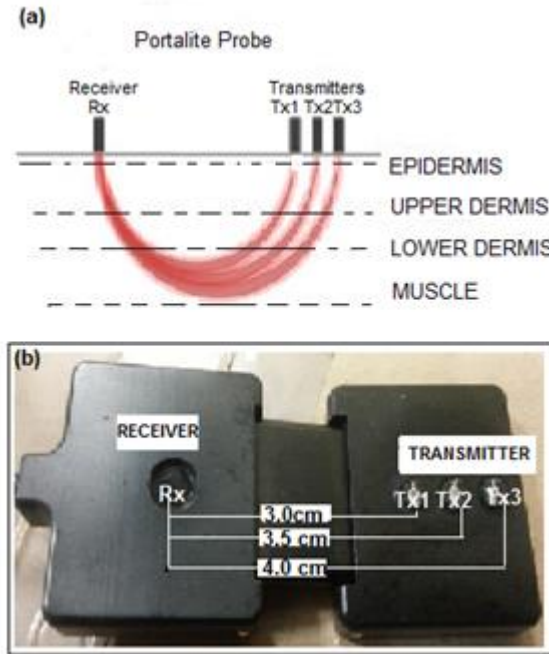


Figure 1: (a) The configuration of Portalite probe fNIRS on human skin; light penetrate and travel into deep layers consists of epidermis, upper dermis, lower dermis and muscle (b) The optode arrangement at 3.0, 3.5 and 4.0 cm of Portalite probe fNIRS on human skin

Figure 1 shows the ‘banana slope effect’ in which the light sources will shine the light into the skin and penetrate half distance of separation sources and detector into tissue layers and reflected back to the detector [11]. This fNIRS device is composed of one detector and three light sources located at three different optode separation at 3cm, 3.5cm and 4cm on sensor allowed to penetrate for approximately 1.5cm, 1.75cm and 2cm into human layers [16][17].

C. Experimental Set up

The experimental protocol used in this study has three parts: adipose tissue thickness (ATT) measurement on target muscle, cuff occlusion before exercise and after each level of exercise (0-50%) and increment of isometric exercise level based on 1RM fatigues level (0-50%).

First of all, the adipose tissue thickness (ATT) was measured on target muscle using a skin-fold caliper. Repeated measurements around the target muscle were taken using this caliper. ATT was measured as a mean value and results are given in millimeters (mm).

Before the experiment begins, electronics dynamometer handgrip was used to obtain 1RM value. A sphygmomanometer cuff was placed loosely around the upper arm in order for arterial occlusion (AO) to be applied as part of the experiment. Although the sensor in the instrument incorporates an ambient light filter, the forearm was covered by an opaque cloth to avoid any possibility of signal contamination by ambient light.

Repetition numbers of contraction for each volunteer are varied based on their strength and fatigues level [11]. Fatigues levels are composed of three different levels of exercise starting from 0%, 10%, 30% and 50%.

Immediately after each exercise intensities period within 0-120 s, an arterial occlusion (AO) at 200mmHg was applied for 60sec to measure the oxygen consumption used based on oxygenated and deoxygenated hemoglobin and myoglobin signal.

Each activity lasted at every AO for 60 seconds, followed by 60 seconds of resting period between exercises in order to allow the hemodynamic activations with fNIRS to return to a zero baseline value. AO required a pneumatic cuff on the forearm by inflating the cuff to a given pressure at 200 mmHg [11]. During arterial occlusion (AO), both arterial and venous are blocked [11]. At this state, the deoxygenated hemoglobin and myoglobin [HHb+Mb] increase while oxygenated hemoglobin [HbO2+MbO2] decrease thus resulting in constant blood volume because of no blood flow during this condition [11].

Repeated step for AO measurement for other two level of exercise (30% and 50%). The subjects will be asked to relax in order to get the baseline fNIRS signal before applying a final occlusion. Lastly, post-AO was conducted at the end of recovery to get final oxygen consumption within muscle after recovery for maximal exercise intensity.

Experimental set up can be illustrated in Figure 2.

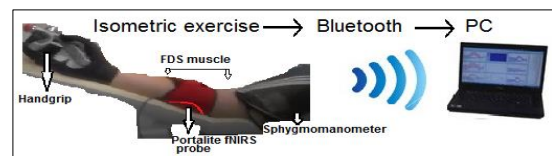


Figure 2: Probe and forearm position in this study

Figure 2 above shows the set up the arrangement of human forearm approximately 30 degrees [18] from the ground level in order to avoid venous pooling of the blood [19]. The overall time series is shown in Figure 3 below:

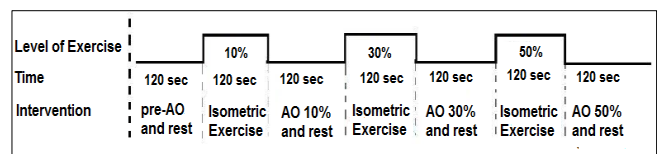


Figure 3: Time series paradigm protocols task for each volunteer

The whole experimental protocols time series task for each volunteer is shown in Figure 3.

D. Intervention Analysis

The modified Beer-Lambert law was applied and express in term of optical density (OD) as below:

$$OD(\lambda) = \epsilon(\lambda) \cdot C \cdot L \cdot DPF + OD(\lambda)_R \tag{1}$$

Where OD(λ) is optical density as a function of wavelength (760 nm and 830 nm) for each chromophore, OD(λ)_R constant value for all volunteers and a dimensionless path-length correction factor based on Deply et al. [20] and (DPF) is differential path-length factor (DPF=4) [11] as suggested by the manufacturer for the muscle. ε(λ) is the extinction coefficient also as a function of wavelength of the chromophores (mM⁻¹.cm⁻¹), C is the concentration of

chromophores (Mm), L is the separation distance between source and detector which varied based on optode position. $OD(\lambda)_R$ was assumed to be constant at all period so that concentration $[\Delta C]$ equation can be derived as below:

$$[\Delta C] = \frac{\Delta OD(\lambda)}{\epsilon(\lambda)L.DPF} \quad (2)$$

This concentration from all the hemodynamic signal of oxygenated, deoxygenated and a total of hemoglobin [Hb] and myoglobin [Mb] based on Equation (2) can be obtained by this device. Pre-AO and each post-AO testing intervention comparison were evaluated in this study. Pearson's correlation analysis was used to compare the correlation between optical measure by each channel and level of exercise from 0% to 50%. In addition, gender analysis also was evaluated using the multivariate graph and Pearson correlation coefficient. The level of statistical significance was set at $p \leq 0.05$.

III. RESULT AND DISCUSSION

A. Relationship between hemodynamics signal and channels

fNIRS consists of three different optode separation which is the first optode separation at 3.0 cm followed by second optode separation at 3.5 cm and third optode separation at 4.0 cm. The first optode separation (3 cm) and third optode separation (4.0 cm) had shown higher changes on activities compare to the second optode separation (3.5 cm).

The result in Figure 4 shows the obvious changes occurrence on optode's channel:

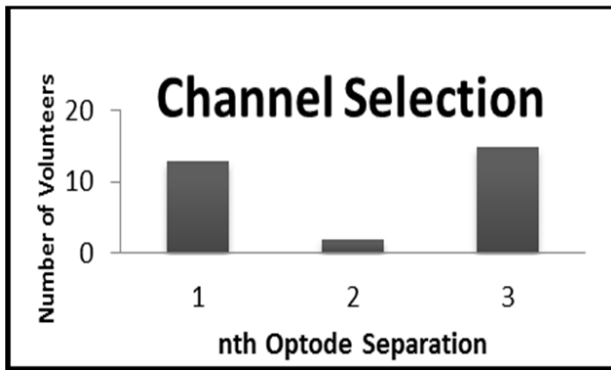


Figure 4: Optode Separation Selection

Based on Figure 4, the first optode separation (3 cm) and third optode separation (4.0 cm) had shown higher changes on activities compare to the second optode separation (3.5 cm). It also shows that, most activities are only relying on the first and third optode separation since all volunteers have different adipose tissue thickness (ATT).

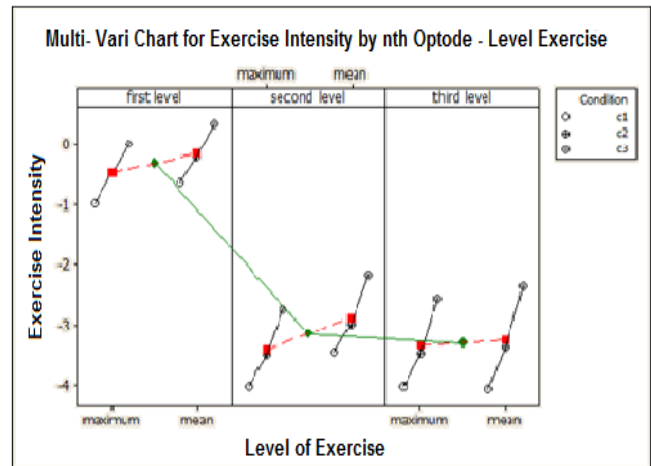


Figure 5: Multivariate chart for the linear regression of exercise intensity changes depending on the level of isometric assessment first level, second level and third level of isometric assessment

The multivariate chart in Figure 5 showed the level of exercise at first, second and third exercise level (10%, 30% and 50%). There is three conditions shown in Figure5, these three condition refers to three channel c1, c2, and c3 located at the different position of optode configuration at 3.0, 3.5 and 4.0 cm. Localized channel analysis, minimum, maximum and mean were analyzed for each peak response of oxygenated hemoglobin and myoglobin [HbO₂ and MbO₂], deoxygenated hemoglobin and myoglobin [HHb and Mb] and total hemoglobin and myoglobin [tHb+tMb] at three different optode separation. Based on Figure 5, all activities showed the detection decrease as increase the distance between source and detector. In addition, the mean signal is more significant to compare these three channels compare to the maximum signal ($p < 0.05$). It is because of slight motion or noises occur during the experiment. Oxygenated and deoxygenated of hemoglobin and myoglobin where then characterize and it is shown that, the oxygen saturation as the level of isometric assessment increase as shown in Figure5 above.

B. Relationship between hemodynamics signal and gender

Balance samples from volunteers then were used to evaluate the correlation between hemodynamics signal and gender through the exercise level from 0-50%. The significant difference was only found from deoxygenated ($p=0.031$) of hemoglobin and myoglobin signal. Meanwhile, no correlation obtained by hemodynamics signal from oxygenated and total of hemoglobin and myoglobin as shown in Table 1.

Table 1
Correlation between hemodynamic signal and gender

Hemodynamics Signal	P-value
Oxygenated hemoglobin and myoglobin	0.081
Deoxygenated hemoglobin and myoglobin	0.031
Total hemoglobin and myoglobin	0.225

Values are measured based on means \pm range signals for all hemodynamic change under three level of isometric exercise.

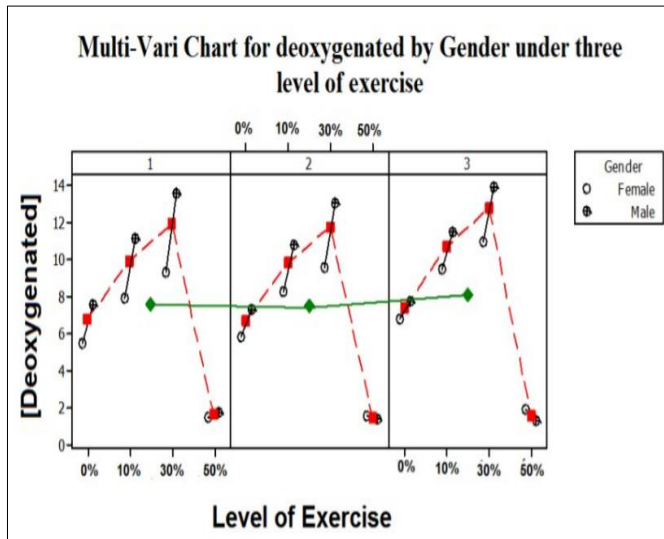


Figure 6: Multi-variate chart for deoxygenated by gender under three level of exercise

Based on Figure 6, there are four level of exercise starting from 0% (pre-AO signal) and followed by a signal after 10%, 30% and 50%. In this Figure, it was separated by three blocks which refer to channel numbering 1(3.0 cm), 2 (3.5 cm) and 3 (4.0 cm) of optode position. According to Figure 6, the oxygenated signal for each channel linearly increase from 0% to 30% but extremely decrease after 30% level of exercise due to fatigue was achieved at that time. At 50% level of exercise, the female shown more fatigues compare than male since the deoxygenated signal for a female is higher than male as shown in Figure 6.

IV. CONCLUSION

As a conclusion, quantitative variations in oxygen saturation can be measured based on the signal of near-infrared light which will reflect the balance of oxygenation level in human muscle. The linear regression slope for 0%-10% is drop then oxygen level moderately drops after 30%-50% level of isometric exercise. In this gender analysis study, the deoxygenated hemoglobin and myoglobin show more significant when compared to the oxygenated hemoglobin and myoglobin. In this study, it also is shown that the oxygenated hemoglobin myoglobin [HbO₂ and MbO₂] is increased if the muscle is used because the oxygen is consumed there and more oxygen is demanded especially in female compare in the male. We hope that this preliminary study could help more investigation and other scientific community of muscle physiology in future.

ACKNOWLEDGMENT

This study was supported by Science Fund Grant (06-03-04-SF0057) from the Ministry of Science and Technology.

REFERENCES

- [1] J. E. Peltonen, J. M. Kowalchuk, D. H. Paterson, D. S. DeLorey, G. R. DuManoir, R. J. Petrella, and J. K. Shoemaker, "Cerebral and Muscle Tissue Oxygenation in Acute Hypoxic Ventilatory Response Test," *Respir. Physiol. Neurobiol.*, vol. 155, no. 1, pp. 71–81, Jan. 2007.
- [2] A. A. A. Halim, M. H. Laili, N. A. Aziz, A. R. Laili, M. S. Salikin, and M. Rusop, "A Review on the Non-Invasive Evaluation of Skeletal Muscle Oxygenation," *Am. Inst. Phys.*, vol. 020011, no. 1733, pp. 1–6, 2016.
- [3] E. M. C. Hillman, "Experimental and Theoretical Investigations of Near Infrared Tomographic Imaging Methods and Clinical Applications," 2002.
- [4] M. Angela, E. Gratton, D. Hueber, and S. Fantini, "Near-Infrared Absorption and Scattering Spectra of Tissues in Vivo," *SPIE Opt. Tomogr. Spectrosc. Tissue III*, vol. 3597, pp. 526–531, 1999.
- [5] R. Morhard, H. Jeffery, and A. McEwan, "Simulation-Based Optimization of a Near-Infrared Spectroscopic Subcutaneous Fat Thickness Measuring Device," *Conf. Proc. ... Annu. Int. Conf. IEEE Eng. Med. Biol. Soc. IEEE Eng. Med. Biol. Soc. Annu. Conf.*, vol. 2014, pp. 510–513, Jan. 2014.
- [6] Y. Yang, M. A. Shear, O. O. Soyemi, and B. R. Soller, "Effect of Skin and Fat Layers on the Spatial Sensitivity Profile of Continuous Wave Diffuse Reflectance Near Infrared Spectra," *Smart Med. Biomed. Sens. Technol. III*, vol. 6007, p. 60070M, 2005.
- [7] D. Jurovata, J. Kurnatova, S. Ley, D. Laqua, P. Vazan, and P. Husar, "Simulation of Photon Propagation in Tissue using MATLAB," *Int. Dr. Semin.*, 2013.
- [8] A. Shaharin, "Photon Time of Flight and Continuous Wave Near Infrared Spectroscopy of Human Skeletal Muscle Tissue; A Comparative Study," 2013.
- [9] B. Nasouri, "Near Infrared Laser Propagation and Absorption Analysis in Tissues Using Forward and Inverse Monte Carlo Methods," 2014.
- [10] B. Chatel, D. Bendahan, and T. Jue, "Hemoglobin and Myoglobin Contribution to the NIRS Signal in Skeletal Muscle," in *Modern Biophysics*, 2017, pp. 109–117.
- [11] A. A. A. Halim, M. H. Laili, N. A. Aziz, A. R. Laili, M. S. Salikin, and M. Rusop, "Evaluation of Muscle Oxygen Consumption at Regional Level of Fatigue using Functional Near Infrared Spectroscopy," *IEEE 6th Int. Conf. Photonics*, vol. 2016, no. 6, pp. 1–3, 2016.
- [12] A. Macnab and B. Shadgan, "Biomedical Applications of Wireless Continuous Wave Near Infrared Spectroscopy," *Biomed. Spectrosc. Imaging*, vol. 1, no. 3, pp. 205–222, 2012.
- [13] F. Scholkmann, S. Kleiser, A. J. Metz, R. Zimmermann, J. Mata Pavia, U. Wolf, and M. Wolf, "A Review on Continuous Wave Functional Near-Infrared Spectroscopy and Imaging Instrumentation and Methodology," *Neuroimage*, vol. 85, no. 1, pp. 6–27, Jan. 2014.
- [14] D. D. S. Dias, "Design of a Low-Cost Wireless NIRS System with Embedded Linux and a Smartphone Interface," 2015.
- [15] M. J. Khan, K. S. Hong, N. Naseer, and M. R. Bhutta, "A Hybrid EEG-fNIRS BCI: Motor Imagery for EEG and Mental Arithmetic for fNIRS," *Int. Conf. Control. Autom. Syst.*, vol. 2014, no. 14, pp. 275–278, 2014.
- [16] K. Svanberg, "Non-Invasive Optical Monitoring of Free and Bound Oxygen in Humans," 2016.
- [17] M. C. P. Van Beekvelt, M. S. Borghuis, B. G. M. Van Engelen, R.A. Wevers, and W. N. J. Colier, "Quantitative Near Infrared Spectroscopy in Human Skeletal Muscle," *Biochem. Soc. Med. Soc.*, vol. 101, pp. 21–28, 2001.
- [18] M. C. P. V. A. N. Beekvelt, W. N. J. M. Colier, R. O. N. A. Wevers, and B. G. M. V. A. N. Engelen, "Performance of Near-Infrared Spectroscopy in Measuring Local O₂ Consumption and Blood Flow in Skeletal Muscle," *J. Appl. Physiol.*, vol. 90, no. 2001, pp. 511–519, 2001.
- [19] B. Shadgan, W. D. Reid, R. Gharakhanlou, and L. Stothers, "Wireless Near-Infrared Spectroscopy of Skeletal Muscle Oxygenation and Hemodynamics during Exercise and Ischemia," *Spectroscopy*, vol. 23, pp. 233–241, 2009.
- [20] D. DT, C. M, van der Z. P, A. S, W. S, and W. J., "Estimation of Optical Pathlength Through Tissue From Direct Time of Flight Measurements," *Phys. Med. Biol.*, vol. 33, no. 12, pp. 1433–1442, 1988.